Title: **Crystal structure of the *V. parahaemolyticus* ToxS dimer suggests a model for bile-induced ToxRS activation**

Authors: Minje Kim, F. Jon Kull, Charles R. Midgett*

Affiliations:

Department of Chemistry, Dartmouth College, Hanover, NH, USA

*Corresponding author: Charles R. Midgett; charles.r.midgett@dartmouth.edu

Crystal structure of the *V. parahaemolyticus* ToxS dimer suggests a model for bile-induced ToxRS activation

Minje Kim, F. Jon Kull, Charles R. Midgett*
Department of Chemistry, Dartmouth College, Hanover, NH, USA

*To whom correspondence should be addressed. charles.r.midgett@dartmouth.edu

Abstract

The ToxRS system is a member of a two-protein transmembrane transcriptional regulator family of proteins that act as critical environmental stress sensors and regulate virulence gene expression in some bacterial pathogens. These systems are thought to operate by sensing environmental stimuli and transmitting signals through periplasmic domains to activate DNA-binding transcription factors. In *Vibrio parahaemolyticus* and *Vibrio cholerae*, the ToxRS system regulates virulence factors responsible for severe gastrointestinal symptoms in humans. ToxS has been shown to modulate the activity of its binding partner ToxR by binding bile salts, antimicrobial cholesterol metabolites secreted into the human gut. However, the molecular mechanism underlying this regulation is unclear. Here, we present the crystal structures of the *V. parahaemolyticus* ToxS periplasmic domain (ToxSp) with and without the bile salt glycocholate. ToxSp forms an 8-stranded broken β-barrel with a central α-helix and is structurally homologous to a group of chaperone proteins. Notably, the glycocholate-bound ToxSp structure forms a strand-swapped homodimer containing three bound glycocholate molecules. Modeling two ToxR periplasmic domains in complex with the glycocholate-bound ToxSp dimer provides a structure-based model for bile salt activation of the ToxRS system and suggests that ToxRS homologs may be regulated in a similar manner across diverse bacterial species.

Introduction

Many pathogenic bacteria utilize the family of co-component transmembrane transcription regulators (coTTR) to regulate pathogenesis in response to host signals (Demey et al., 2023). These include VtrAC as well as ToxRS from *Vibrio* spp., PsaEF from *Yersinia* spp., GrvA-FidL from enterohemorrhagic *Escherichia coli*, and YqeIJ from avian pathogenic *E. coli* (Herrington et al., 1988; Hubbard et al., 2016; P. Li et al., 2016; K. A. Miller et al., 2016; J. K. Morgan et al., 2015; Quinn et al., 2019; Xue et al., 2020).

These two-protein systems are thought to form obligate heterodimers where they modulate gene expression in response to host signals for survival and colonization (Demey et al., 2023; Kinch et al., 2022). This is thought to occur by the binding partner sensing a stimulus, binding a small molecule, and then passing the signal to the transcription factor through their respective periplasmic domains (V. J. DiRita & Mekalanos, 1991; Kinch et al., 2022; P. Li et al., 2016). As the structure of VtrAC bound to activating bile salt and the apo VtrAC structure were largely the same, how signal sensing leads to transcription factor DNA binding is still unknown (Gotoh et al., 2010; P. Li et al., 2016).

Each protein pair in this family is composed of a transmembrane transcription factor with an N-terminal winged helix-turn-helix DNA-binding domain followed by a transmembrane helix and a C-terminal periplasmic domain, and its periplasmic binding partner that has a short N-terminal tail followed by a transmembrane helix and a C-

terminal periplasmic domain (Canals et al., 2023; Demey et al., 2023). While the periplasmic domains of these proteins have little sequence homology between family members, many are clearly structural homologs (Gubensäk et al., 2023; P. Li et al., 2016; Midgett et al., 2020).

ToxRS is conserved across the Vibrionaceae family where it has been shown to act as an environmental sensor (Lee et al., 2000; Reich & Schoolnik, 1994; Welch & Bartlett, 1998). Most notably, in several *Vibrio* spp. ToxRS protects against the antimicrobial effects of bile salts, cholesterol metabolites produced in the liver and secreted into the intestine (Provenzano et al., 2000). In addition, in some Vibrionaceae family members ToxRS regulates various virulence factors (Hubbard et al., 2016; Lee et al., 2000; V. L. Miller & Mekalanos, 1984). In *V. cholerae* ToxRS helps mediate the stress response to bile salts by binding to the promoters of the outer membrane porins, OmpU and OmpT, regulating their transcription (Crawford et al., 1998; C. C. Li et al., 2000). ToxRS works with another coTTR pair, TcpPH, to activate virulence via the transcription of *toxT* (Beck et al., 2004; Crawford et al., 2003; S. J. Morgan et al., 2011). ToxT directly promotes the transcription of the cholera toxin and toxin co-regulated pilus genes that are required to cause disease (V. DiRita et al., 1991; Higgins & DiRita, 1994; Krukonis et al., 2000; Withey & DiRita, 2006). Similarly, in *V. parahaemolyticus* ToxRS regulates bile response and works with another coTTR pair, VtrAC, to promote the expression of *vtrB*, which activates transcription of the genes required for the type III secretion system (Hubbard et al., 2016; Provenzano et al., 2000).

While much research has focused on the role of ToxR in these processes, it is clear ToxS is an equally important member of this complex. This was demonstrated in mouse model colonization studies using Δ*toxS* strains of both *V. cholerae* and *V. parahaemolyticus,* which were deficient in colonization compared to the wild type bacteria (Hubbard et al., 2016; Pearson et al., 1990). These defects in colonization may reflect the underlying processes that ToxS influences. For example, ToxS can stabilize ToxR in a conformation that induces the formation of an intra-chain disulfide bond, reducing ToxR proteolysis (Lembke et al., 2018). In addition, it has been observed that a Δ*toxS* strain underwent ToxR proteolysis in nutrient-limiting or alkaline conditions, while in the wild type strain ToxR is proteolyzed only when both conditions were present (Almagro-Moreno et al., 2015). Finally, ToxS is required for full ToxR activity in response to several stimuli including bile salts (V. J. DiRita & Mekalanos, 1991; Fengler et al., 2012; V. L. Miller et al., 1989), as in minimal media, ToxR requires ToxS to respond to bile salts and the amino acid mixture NRES (Mey et al., 2012; Midgett et al., 2017). These studies lead to the hypothesis that ToxRS acts as a system that has on and off states, with the presence of ToxS required for full activity (Mey et al., 2012; Midgett et al., 2017).

To understand how ToxS influences ToxR in the presence of bile salts, we solved the structure of the apo and glycocholate-bound ToxS periplasmic domain (ToxSp) from *V. parahaemolyticus* (Vp-ToxSp). ToxSp was monomeric in the apo state and dimeric in the bile salt-bound state, suggesting ToxS directly senses environmental stress signals and dimerizes upon ligand binding. Additionally, a structural analysis of ToxSp suggests it is related to a group of chaperone proteins. These results suggest that coTTRs are activated by interacting with environmental stimuli, leading to heterotetramer formation and DNA binding.

Results

The ToxS periplasmic domain forms a broken β-barrel structure. We solved the structure of a *V. parahaemolyticus* ToxS periplasmic domain, residues Ser25-Asn171 (Vp-ToxSp) (**Table S1**). Overall, the domain is composed of an eight-stranded broken β-barrel (**Figure 1**). The domain begins with the N-terminal helix, α1, which sits at the base of the β-barrel and would be proximal to the membrane. This is followed by five β-strands, a second α-helix, and three final β-strands. In the apo structure, several of the loops connecting the β-strands are disordered. One distinguishing feature, discussed below, is a groove that has been proposed to be the binding site for small molecules (Gubensäk et al., 2023).

The central core of Vp-ToxSp has a combination of hydrophobic and hydrophilic regions. The membrane-distal region of the apo Vp-ToxSp structure contains a solvent-accessible pocket, similar to one observed in VtrC and in the *V. cholerae* ToxRS structure (Gubensäk et al., 2023; P. Li et al., 2016; Zou et al., 2023), suggesting bile salts will bind to Vp-ToxSp in the same manner as they do in VtrC (Gubensäk et al., 2023; Zou et al., 2023). The pocket extends towards the membrane, with the top flanked by hydrophobic residues, a central hydrophilic ring, and a hydrophobic cavity that is sealed by α1 (**Figure 2**).

ToxS sequence conservation. To examine the amino acid conservation, 280 ToxR sequences from the Vibrionaceae family were aligned using UniPro UGENE (Okonechnikov et al., 2012), and the corresponding ToxS sequences were arranged in the same order. Both sets were analyzed using Clustal Omega from the EMBL server to generate a percent identity matrix (**Figure S1, S2**) (Sievers et al., 2011). Examining both matrices showed that the ToxSp periplasmic domain is more conserved than the ToxR periplasmic domain and that the sequence groupings observed for ToxSp sequence alignment are similar to those seen in the ToxRp alignment.

Using the alignment discussed above, we used ChimeraX to assess sequence conservation (Pei & Grishin, 2001). The most conserved residues are in the hydrophobic core, with three residues being 100% conserved, Trp37, Gly99, and Trp101 (**Figure 3**). The two tryptophan residues insert into the hydrophobic core, and Gly99 appears to be important for forming a kink in β4, influencing the positioning of Trp101. In contrast, none of the residues surrounding the ligand-binding pocket (**Figure 3**) have 100% identity, with low identity across the Vibrionaceae family. However, many pocket residue positions show a preference for hydrophobic side chains (**Table S2**). For example, several pocket residues are predominantly hydrophobic across the alignment (>90%), while others retain hydrophobic character in about 70% of the sequences. Together, this suggests that ToxS is built from a conserved hydrophobic core and that it binds hydrophobic ligands through nonspecific interactions in the pocket. The ToxS/ToxR binding interface also has low sequence identity, indicating ToxS and ToxR have undergone coevolution at their binding interfaces.

The ToxS periplasmic domain fold is related to a large group of chaperones. We performed a DALI search to identify proteins with structures similar to ToxSp (**Table S3**) (Holm & Laakso, 2016). The results showed several proteins containing an 8-stranded broken β-barrel structure, including MxiM from *Shigella flexneri*, and HslJ (PDB ID: 2KTS) first identified in *Escherichia coli* (**Figure 4**) (Lario et al., 2005; Lilic et al., 2003; Okon et al., 2008). Additional structural similarity was observed with an AlphaFold-predicted structure of META1, part of the META family in *Leishmania* spp. (Puri et al., 2011).

All of these proteins function in some manner as chaperones — ToxS enhances the stability and may enhance disulfide bond formation of the ToxR periplasmic domain (Ottemann & Mekalanos, 1996; Pfau & Taylor, 1998).

MxiM is an outer membrane associated pilot protein for a type III secretion system that is required to translocate proteins necessary to invade cells in culture in *Shigella* spp. (Schuch & Maurelli, 1999). HslJ is a stress-induced periplasmic chaperone found in a number of bacterial species (Fränzel et al., 2012; Gao et al., 2022; Lilic et al., 2003; Scribano et al., 2019, 2025). While the role of META1 is not clear, overexpression of META1 in *L. amazonensis* leads to increased virulence in mice (Puri et al., 2011; Schuch & Maurelli, 2001; Scribano et al., 2025). Furthermore, another META domain containing protein in *L. amazonensis* META2 is upregulated in response to heat shock and oxidative stress (Ramos et al., 2011). Despite their structural and functional similarities, ToxS, HslJ, MxiM, and META1 families have very limited sequence homology (Puri et al., 2011).

Vp-ToxSp bound to bile salts is dimeric. The 1.9 Å crystal structure of Vp-ToxSp bound to glycocholate reveals a dramatic ligand-induced conformational change when compared to the apo form (**Figure 5A; Table S1**). Each monomer from the dimer shows the same 8-stranded broken β-barrel fold with the two α-helices in the same positions, but the bile salt bound structure forms a dimer with the two monomers exchanging their β8 strands (**Figure 5B, 5C**). The swapped β8 strands align in the same register as in the apo form, preserving the hydrogen-bonding pattern of the β-barrel. In contrast to the apo form, all the loops at the top of the structure are resolved, with the loop between β1 and β2 folding over the top of the barrel, capping the binding pocket (**Figure 5A**). The orientation of the N-termini of the two monomers in the dimer would accommodate adjacent transmembrane helices inserting into the membrane (**Figure 5A**).

Three glycocholate molecules are bound to the ToxSp dimer. The strand-swapped ToxSp dimer structure contains three glycocholate molecules bound between the two ToxSp monomers toward the top of the β-barrel. In each monomer, glycocholate binds the hydrophobic pocket formed by residues from β1, β2, β3, and α2 (**Figure S3A**). The middle glycocholate is bound in a pocket formed by the C-terminal end of α2 from the two monomers. The glycocholates are arranged with their hydrophobic ring side binding to the upper hydrophobic region of the pocket and their polar hydroxyl and glycine groups exposed to the solvent (**Figure 5A, 5B**). The third, central glycocholate bridges the two glycocholate molecules. Binding contacts from each monomer are not identical due to the asymmetric contacts at the interface. In addition to the ligands within the dimer, two glycocholate molecules are observed at the crystal packing interfaces. These both have weaker density and are unlikely to be physiologically relevant (**Figure S3B**).

The extended binding pocket observed in the ToxSp dimer is absent in the apo structure, suggesting a model where binding of the three glycocholate molecules drives the dimerization of ToxSp, which is further stabilized by the swapping of the β8 strands. ToxS is thus acting as a sensor that, upon binding bile, transitions from a monomer to a domain-swapped dimer. This appears to be a key step in the activation of the ToxRS system.

ToxS and VtrC bind bile in different ways. Comparison of bile salt-bound VtrC and ToxSp shows that in VtrC taurodeoxycholate and chenodeoxycholate bind similarly in a pocket formed by the β-barrel domain (P. Li et al., 2016; Zou et al., 2023). In ToxSp, helix α2 occupies the position where the bile salt sits in the VtrC structure (**Figure 6**). In addition, the β1-β2 loop that closes over the top of the ToxSp barrel is absent in VtrC. Therefore, the orientation of the ligand is also different, with the side chain of glycocholate in ToxSp projecting outward, rather than upward in VtrC (**Figure 6**). The outward orientation of the glycine group of the glycocholate exposes the hydrophilic tail to solvent and potentially allows recognition of bile salts with diverse side chains. This suggests that, while ToxS and VtrC share an overall broken β-barrel fold, ToxS may bind a variety of ligands, consistent with its role as a general sensor. The different ligand binding modes observed in

ToxS and VtrC suggest that different coTTR binding partners have developed unique ways to bind bile, while maintaining the overall broken β-barrel structure.

ToxSp bound to bile resembles ToxS in the ToxR-bound state. Comparison of the *V. parahaemolyticus* ToxSp structures (apo and glycocholate-bound) with the *V. cholerae* ToxSp (Vc-ToxSp) from the heterodimeric ToxRS complex shows that bile salt binding of ToxSp induces structural changes similar to those observed in the ToxR-bound conformation (**Figure 7**) (Gubensäk et al., 2023). In apo Vp-ToxSp, the β1 strand of the barrel is bent inward, with a single water molecule bridging β1 and β8, resulting in a more closed conformation, consistent with no ligand or binding partner present (**Figure 7A**). However, the glycocholate-bound Vp-ToxSp structure is more open, with two waters between β1 and β8 strands, similar to Vc-ToxSp bound to ToxR, where the side chain of Thr279 of ToxR is in a position similar to the two waters in glycocholate-bound Vp-ToxSp (**Figure 7B, C**). Therefore, bile salt binding appears to prepare ToxS for partner binding by inducing a more open conformation of the β-barrel, allowing subsequent ToxR binding. This observation is also consistent with previous work showing that bile salts and Triton X-100 can increase the binding of the ToxRp to ToxSp (Provenzano et al., 2000). In summary, bile salt binding by ToxSp provides a direct mechanism, not only for ToxS dimerization, but also for triggering ToxRS complex formation.

Discussion

In this study, we have reported crystal structures of ToxSp in apo and glycocholate-bound forms and hypothesize that bile-binding induces dimerization of ToxS and formation of a ToxRS heterotetramer. While ToxS has previously been characterized as a member of the lipocalin protein family, our analysis of the ToxSp topology and structure shows that it closely resembles chaperone proteins including HslJ (PDB ID: 2KTS), META1, and MxiM (Lario et al., 2005; P. Li et al., 2016; Okon et al., 2008; Puri et al., 2011; Schaeffer et al., 2025). Like ToxS, these proteins stabilize their partner complexes and respond to stress. HslJ is expressed and secreted into the periplasm when bacteria encounter stressful conditions (Lilic et al., 2003; Scribano et al., 2025). MxiM acts as a pilot protein for the type III secretion system in *Shigella* spp. (Lario et al., 2005; Okon et al., 2008). The META family is thought to play a role in secretion in *Leishmania* spp. (Puri et al., 2011). The common localization in the periplasm and shared structure and topology of these proteins suggests that ToxS and other coTTR proteins have evolved to function as periplasmic chaperones with divergent specific cellular roles and ligands (Kinch et al., 2022).

In addition to the topological analysis, the sequence conservation analysis of the ToxRS periplasmic domains shows ToxS is more conserved across the species than ToxR. In addition, the alignments support the idea that there has been a certain amount of co-evolution with ToxR (**Figure S2 and S3**). The most highly conserved residues are in the hydrophobic core, proximal to the membrane, suggesting that maintaining a stable, broken β-barrel fold is crucial for ToxS function. In contrast, while the specific residues surrounding the ligand-binding pocket vary, their hydrophobic and hydrophilic natures are preserved across the Vibrionaceae family (**Table S2**), allowing the binding of various hydrophobic compounds, as demonstrated by ToxR being activated by several bile salts, interactions between ToxRp and ToxSp increasing in the presence of Triton X-100, as well as studies showing that SDS induces ToxR activity (Midgett et al., 2017; Provenzano et al., 2000).

One of the key questions regarding coTTR systems is how environmental signals activate transcriptional responses. In general, it has been thought that the periplasmic domain senses environmental stimuli and signals through the periplasmic binding interface to the cytoplasmic DNA-binding domain, which then binds

DNA (V. J. DiRita & Mekalanos, 1991; P. Li et al., 2016). For both ToxRS and VtrAC, it has been proposed that the heterodimer binds bile salts (Gubensäk et al., 2023; P. Li et al., 2016). However, our structure of GCH-bound ToxSp shows that ToxS alone can bind bile and induce dimerization; a ToxRS heterodimer is not required for bile recognition. Because ligands and swapped strands are absent in the monomeric apo form, bile salt binding appears to be the driving force for ToxS dimerization.

To investigate how bile-binding activates ToxR, we modeled the ToxR periplasmic domain onto the GCH-ToxSp dimer structure. An alignment of two copies of ToxRp from the *V. cholerae* heterodimeric ToxRS periplasmic domain structure onto each chain in our GCH-ToxSp structure (Gubensäk et al., 2023) shows that all four N-termini of the subunits would face the same direction, that both domain pairs would be positioned to be near the membrane, and that there are minimal steric clashes between ToxS and ToxR in the modeled heterotetramer (**Figure 8**).

Based on the results presented here and the ToxRS model described above, we propose a mechanism for which bile salts activate ToxRS. First, monomeric ToxS on the membrane binds bile salts, inducing dimerization as well as a conformational change in the β-barrel, opening the space between β1 and β8, making it easier for ToxR to bind ToxS. The ToxRS heterotetramer can then bind to DNA and regulate transcription. Alternatively, if ToxS and ToxR have already formed a heterodimer, bile salt binding to ToxS subsequently induces formation of the ToxRS heterotetramer (**Figure 9**). In either case, this model explains how bile salts function as molecular signals that pair periplasmic sensing to activation of the ToxRS system.

In conclusion, we propose that the binding partner proteins of coTTR systems have evolved as chaperones that stabilize their cognate transcription factors, and binding partner dimerization is critical for full transcriptional activation by these systems. Our structures establish ToxS as a sensory periplasmic chaperone that utilizes a bile salt binding pocket to transmit extracellular information across the membrane, upregulating stress response and virulence. Given the critical role the pocket plays in this mechanism, it is a potential target for small molecule therapeutics to inhibit virulence gene expression.

Experimental Methods

Cloning of *V. parahaemolyticus* ToxS periplasmic domain:

The DNA sequence of the *V. parahaemolyticus* ToxS periplasmic domain (residues S24-N171) [WP_020840240] was codon-optimized and synthesized to include a SapI site, the coding sequence, and a BamHI site, flanked by primer binding sites. The fragment was amplified with PCR, digested with SapI and BamHI restriction enzymes, and purified using the PCR purification kit (Qiagen). The pTYB21 vector (NEB), containing an N-terminal chitin-binding domain intein (CBD-intein) affinity tag, was digested with the same restriction enzymes (SapI and BamHI), treated with calf intestinal phosphatase (CIP; NEB), and purified using the PCR purification kit (Qiagen) (**Table S6**). The ToxSp insert was ligated into the prepared pTYB21 vector using Quick Ligase (NEB), and the ligation products were transformed into *E. coli* DH5α cells (NEB). The transformants were selected on an LB agar plate containing 100 µg/mL carbenicillin and screened by colony PCR for the correct insert size. The selected colonies were grown in small-scale cultures; a portion was stored at -80 °C, while plasmid DNA from the remaining culture was purified using the Miniprep kit (Qiagen). Plasmid sequences were confirmed by Sanger sequencing with primers complementary to the T7 promoter.

Protein Expression and Purification:

The confirmed CBD-ToxSp plasmid was transformed into *E. coli* BL21-CodonPlus (DE3) competent cells (Agilent Technologies). Starter culture was grown overnight at 30 °C in ZYP-0.8G medium supplemented with 200 µg/mL carbenicillin and 25 µg/mL chloramphenicol in a shaking incubator (Studier, 2005). The culture was used to inoculate Terrific Broth Modified media (Fisher Scientific) at a 1:250 ratio, supplemented with 2 mM $MgSO_4$, 200 µg/mL carbenicillin, and 25 µg/mL chloramphenicol. The cells were grown at 37 °C to an OD_{600} of 2-3, induced with 1 mM IPTG, and incubated at 18 °C for 16-20 hours.

The cells were harvested by centrifugation at 4,500 × *g* for 25 minutes at 4 °C and resuspended in lysis buffer (20 mM Tris-HCl pH 8.0, 200 mM NaCl, 1 mM EDTA) containing cOmplete protease inhibitor cocktail tablets (Roche). Lysis was performed by passing the cells through a French press three times, and the lysate was centrifuged at 100,000 × *g* for 45 minutes at 4 °C. The supernatant was filtered through a 0.45 µm filter before purification.

The supernatant was passed over chitin-binding resin (NEB) pre-equilibrated with Tris wash buffer (20 mM Tris-HCl pH 8.0, 200 mM NaCl) to capture the CBD-ToxSp fusion protein. The resin was washed sequentially with 10 column volumes (CV) of high-salt Tris wash buffer (20 mM Tris-HCl pH 8.0, 1 M NaCl) and 20 CV of Tris wash buffer. The resin was rapidly washed with 3 CV of Tris cleavage buffer (20 mM Tris-HCl pH 8.0, 200 mM NaCl, 50 mM DTT, 100 mM PMSF, 500 mM EDTA, cOmplete protease cocktail tablet) to saturate the resin and initiate on-column intein-mediated cleavage of the CBD tag.

The column was incubated at 23 °C for 16-40 hours. Cleaved ToxSp protein was eluted in Tris wash buffer, concentrated using Amicon Ultra 3 kDa molecular weight cut-off (MWCO) centrifugal filters (Millipore), and further purified by size-exclusion column (HiLoad 16/600 Superdex 200 pg, Cytiva) pre-equilibrated with gel filtration buffer (20 mM Tris-HCl pH 8.0, 200 mM NaCl). The purified ToxSp protein solution was concentrated to 9-16 mg/mL, flash-frozen in liquid nitrogen, and stored at -80 °C until crystallization.

Crystallization and Data Collection:

To obtain apo ToxSp crystals, a seeded crystallization method was used to promote the growth of diffraction-quality crystals. First, purified ToxSp protein was concentrated to 16 mg/mL and used to generate initial crystals. These initial ToxSp crystals were grown by combining protein and crystallization solution (100 mM succinic acid pH 6.0, 16% (w/v) PEG 3,350) at a 1:1 ratio in a 96-well, 2-drop MRC plate (Swissci) with NT8 Drop Setter (Formulatrix). The resulting crystals were harvested and stored in 50 µL crystallization solution, then disrupted with a polytetrafluoroethylene seed bead (Hampton Research) to generate a seed stock. This stock solution was serially diluted (1:10 to 1:10,000) and stored at room temperature (23 °C).

For seeded crystallization, purified ToxSp protein was concentrated to 14 mg/mL and seeded by adding the diluted seed stock at a 25:2 (v/v) protein-to-seed ratio. The crystallization trials were set up in the 96-well, 2-drop MRC plates (Swissci) using the NT8 Drop Setter (Formulatrix) with protein-to-reservoir ratios of 1:1 (drop 1) and 1:2 (drop 2), using 96-well sparse matrix crystal screens. Under these conditions, the optimal diffraction-quality apo crystals were obtained from Berkeley crystal screen condition E8 (Rigaku Reagents; 100 mM HEPES pH 7.5, 200 mM sodium malonate dibasic pH 7.0, 20% (w/v) PEG monomethyl ether 2,000). The crystals were cryoprotected with a solution formulated with 70% crystal reservoir solution and 30% glycerol.

The diffraction data were collected at the NSLS-II AMX beamline (Brookhaven National Laboratory) and processed to 2.1 Å resolution with XDS, yielding a space group of P 2_1 2_1 2_1 with unit cell parameters 53.746 58.230 89.456 90.000 90.000 90.000 (**Table S1**) (Kabsch, 2010).

To obtain glycocholate-bound ToxSp crystals, the frozen ToxSp protein stock at 16 mg/mL was thawed and supplemented with 10 mM sodium glycocholate stock prepared in ToxSp buffer (20 mM Tris-HCl pH 8.0, 200 mM NaCl) to achieve final concentrations of approximately 622 μM ToxSp and 3.13 mM sodium glycocholate (1:5 protein-to-ligand ratio). The combined glycocholate-ToxSp solution was incubated overnight at 4 °C with rotation to allow complex formation.

The crystallization plates for the glycocholate-bound complex were set up using the same seeding method as for apo ToxSp. The glycocholate-ToxSp solution was seeded by adding diluted seed stock prepared from apo ToxSp crystals at a 25:2 (v/v) protein-to-seed ratio. The crystallization trials were set up in 96-well, 2-drop MRC plates (Swissci) using 96-well sparse matrix crystal screens. The initial crystal hit was observed from Index crystal screen condition H9 (Hampton Research). The Index H9 condition was optimized to 0.06 M zinc acetate dihydrate and 17% (w/v) PEG 3,350. The crystals were cryoprotected with a solution formulated with 70% crystal reservoir solution and 30% glycerol. The diffraction data were processed to 1.9 Å resolution with autoPROC, yielding a space group of P 2_1 2_1 2_1 and a unit cell of 69.828 92.503 95.805 90.00 90.00 90.00 (**Table S1**) (Vonrhein et al., 2011).

Structure Determination:

The structure of apo ToxSp was determined by molecular replacement using an AlphaFold structure prediction model, truncated to exclude regions with pLDDT under 90 (Jumper et al., 2021). The iterative refinement cycles were performed in Refine from PHENIX, and manual model building was performed in COOT (Emsley & Cowtan, 2004). Structural visualization and analysis were performed in ChimeraX (Pettersen et al., 2004). The final structure was deposited in the Protein Data Bank (PDB ID: 8U2F).

The strand-swapped dimer structure of GCH-bound ToxSp was solved by molecular replacement using a RoseTTAFold All-Atom prediction model generated as a monomer (Krishna et al., 2024). The electron density map clearly indicated a strand swap in the β8 region, confirmed by a composite omit map in PHENIX (Adams et al., 2010). The protein structure and GCH ligands were built using COOT with ligand restraints from the REFMAC library (Emsley & Cowtan, 2004; Vagin et al., 2004). The final structure visualization and analysis were performed in ChimeraX (Pettersen et al., 2004).

Conservation analysis:

To analyze the ToxSp sequence conservation, BLAST was used to find sequences homologous to the *V. cholerae* ToxR periplasmic domain residues 199-294 (Altschul et al., 1990; Sayers et al., 2024). The resulting BLAST sequences were then curated by removing entries that were multispecies alignments, partial sequences, identical sequences, or sequences from the same species that were highly similar, leaving a list of ToxR periplasmic domains primarily representing a single sequence per species. The curated ToxRp sequences were aligned using EMBL-EBI and then used to generate a percent identity matrix with Clustal Omega (Madeira et al., 2024; Sievers et al., 2011). Based on this ToxRp sequence alignment, the corresponding ToxSp sequences from the same species were identified in the NCBI and compiled into the

same order as the aligned ToxRp sequences to preserve one-to-one pairing (Sayers et al., 2024). This procedure resulted in a list of 280 paired ToxR and ToxS sequences. The ToxS sequences were then aligned, and the sequences of the N-terminal tail and transmembrane domain were removed so that only periplasmic domains (ToxSp) were retained. Both the ToxRp and ToxSp sequences were subsequently aligned again, and a percent identity matrix calculated by Clustal Omega without rearrangement of the sequence order (Madeira et al., 2024). Once the alignment was complete, the file with the ToxSp alignment was loaded into ChimeraX to calculate and visualize the protein conservation at the residue level using the built-in program AL2CO (Pei & Grishin, 2001).

Figures

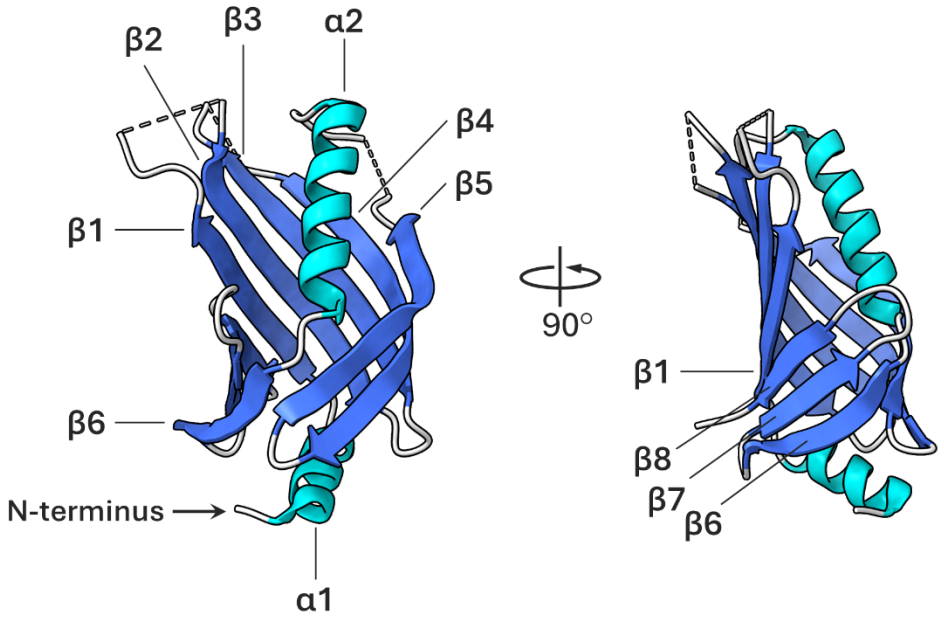

Figure 1. Crystal structure of apo ToxSp. Left; view of the structure showing ToxSp as an 8-stranded broken β-barrel (dark blue) folded around a central helix (cyan). Right; view of the structure showing the C-terminal β-strands β6-β8 interacting with β1.

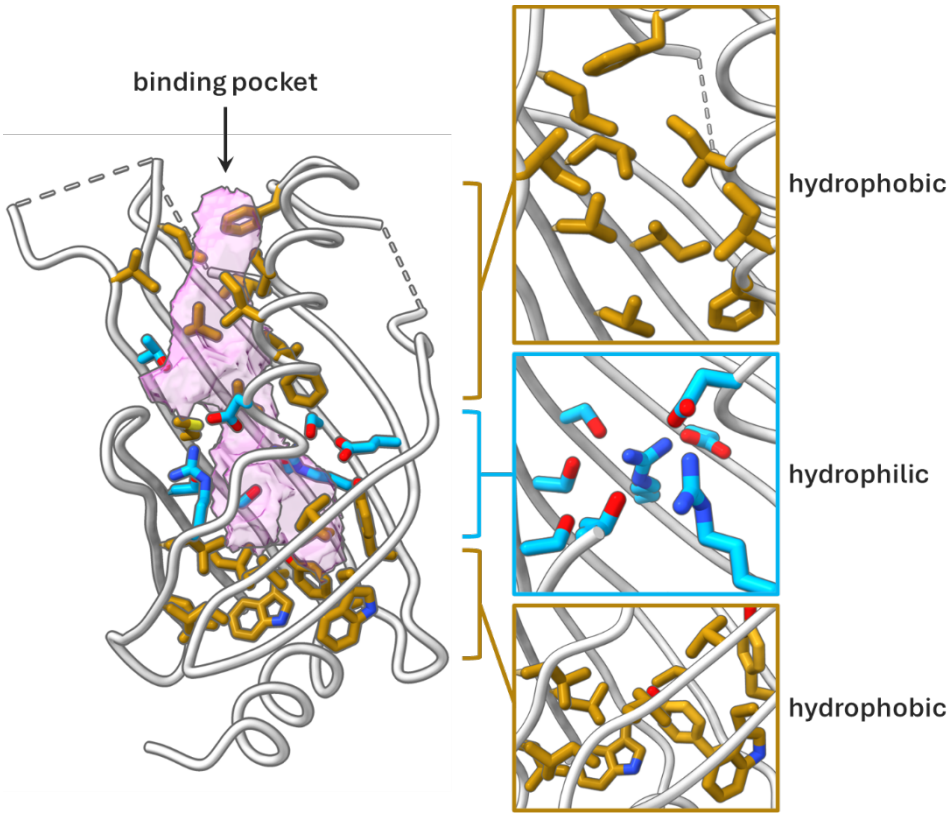

Figure 2. ToxSp contains a binding pocket with alternating hydrophobic and hydrophilic regions. Left; The apo ToxSp structure has a binding pocket (left; pink) enclosed by the β-barrel and the central helix. Right; residues within the binding pocket contain regions of hydrophobic (gold), hydrophilic (blue), and hydrophobic (gold) residues.

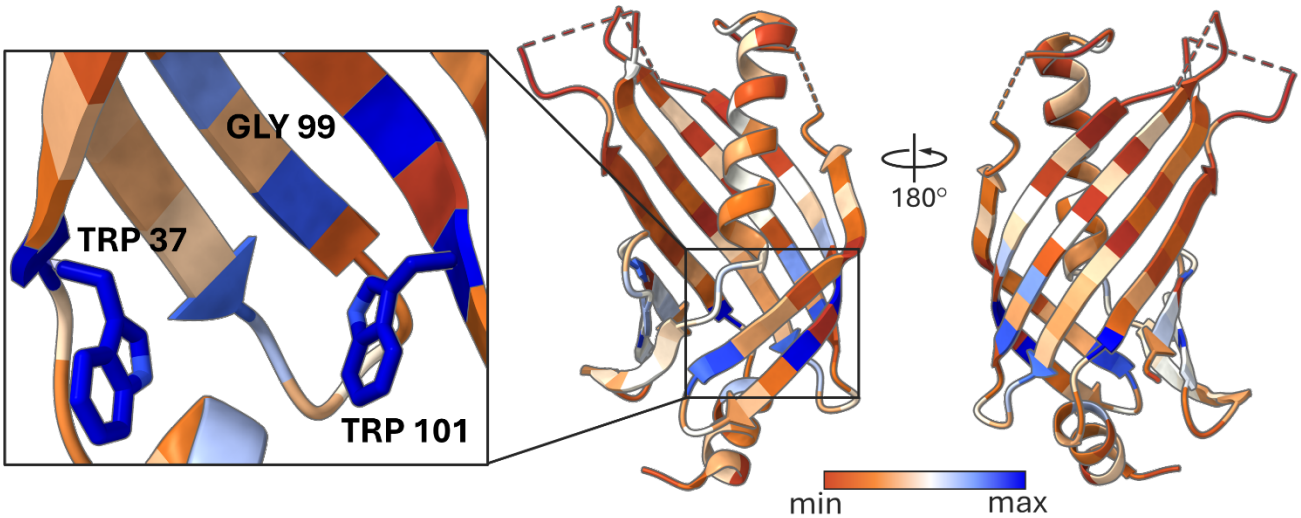

Figure 3. ToxSp conservation displayed on the Apo-VpToxSp structure. Apo Vp-ToxSp structure colored by conservation from sequence alignment across 280 Vibrionaceae family members. Residues Trp37, Gly99, and Trp101 are the only 100% conserved amino acids.

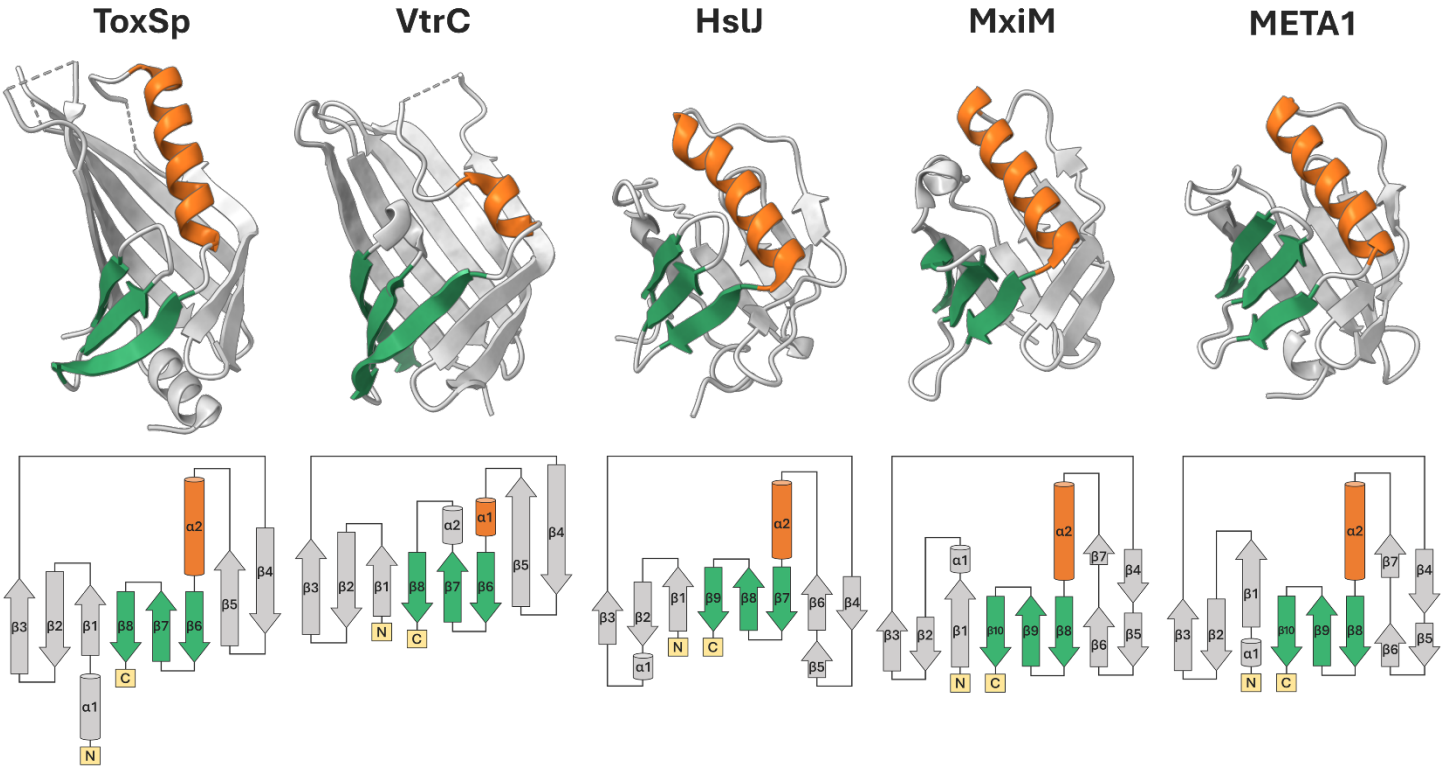

Figure 4. Structure similarity alignment from DALI search reveals that ToxSp is closely related to a large group of chaperone proteins. DALI search result finds several other proteins with structures similar to ToxSp. In addition to VtrC, ToxSp closely resembles a group of chaperone proteins: HslJ (PDB ID: 2KTS), MxiM (PDB ID: 1Y9L), and META1 (AlphaFold). These proteins show both structural and topological similarity as highlighted by the C-terminal β-strands (β6-β8) (green) and central α-helix (orange).

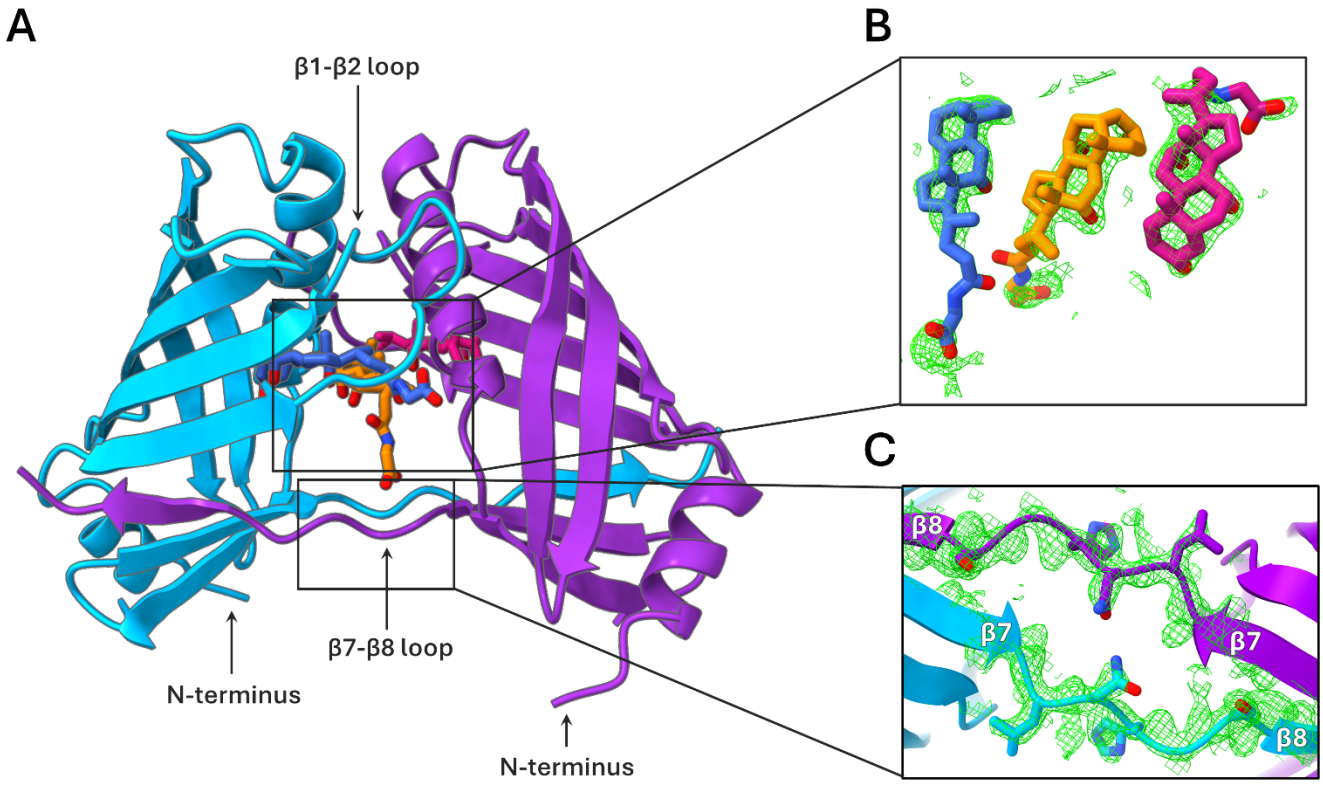

Figure 5. The Vp-ToxSp dimer bound to the bile salt glycocholate. (A) Crystal structure (PDB ID: 9ZJO) of dimeric ToxSp bound to three glycocholate molecules. (B) Electron density map of the three glycocholate molecules bound to the ToxSp dimer displayed as green mesh contoured at 1σ. (C) Electron density map of the crystal structure surrounding the swapped β8 strand loops (Ser160-Thr166) displayed as green mesh contoured at 1σ with β7 and β8 labeled.

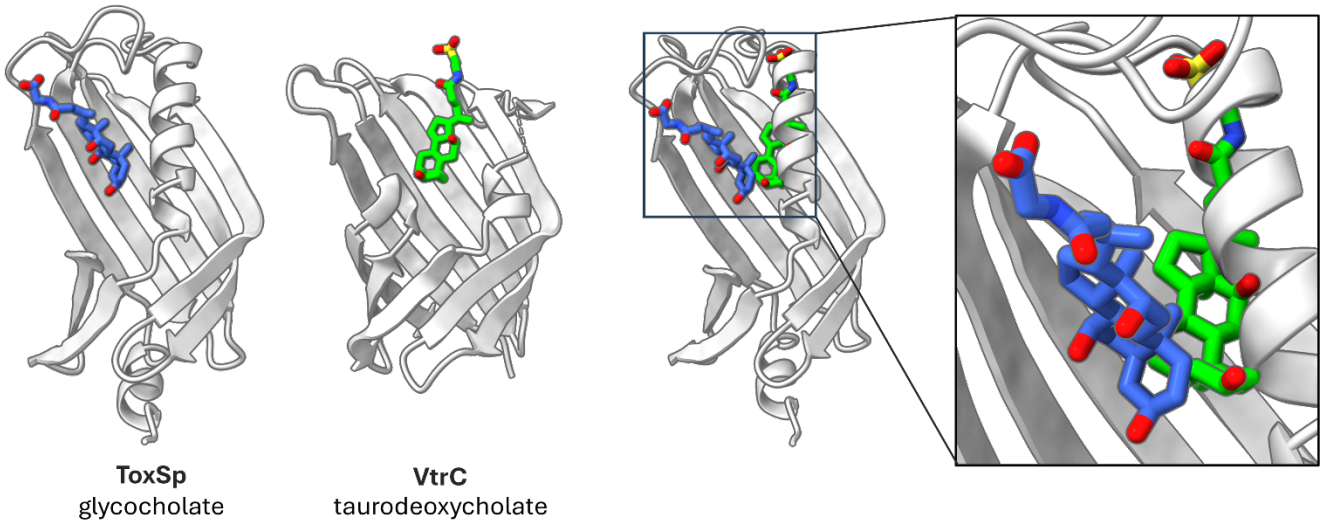

Figure 6. ToxSp and VtrC are structurally homologous with different bile salt binding positions and orientations. Left; A monomer of Vp-ToxSp bound to glycocholate. Middle; VtrC bound to taurodeoxycholate (PDB ID: 5kew, green). Right; Overlay of the crystal structures of glycocholate-bound Vp-ToxSp monomer (PDB ID: 9ZJO, blue), and taurodeoxycholate bound to VtrC (not shown) with a close-up showing differences in the bile salt orientations.

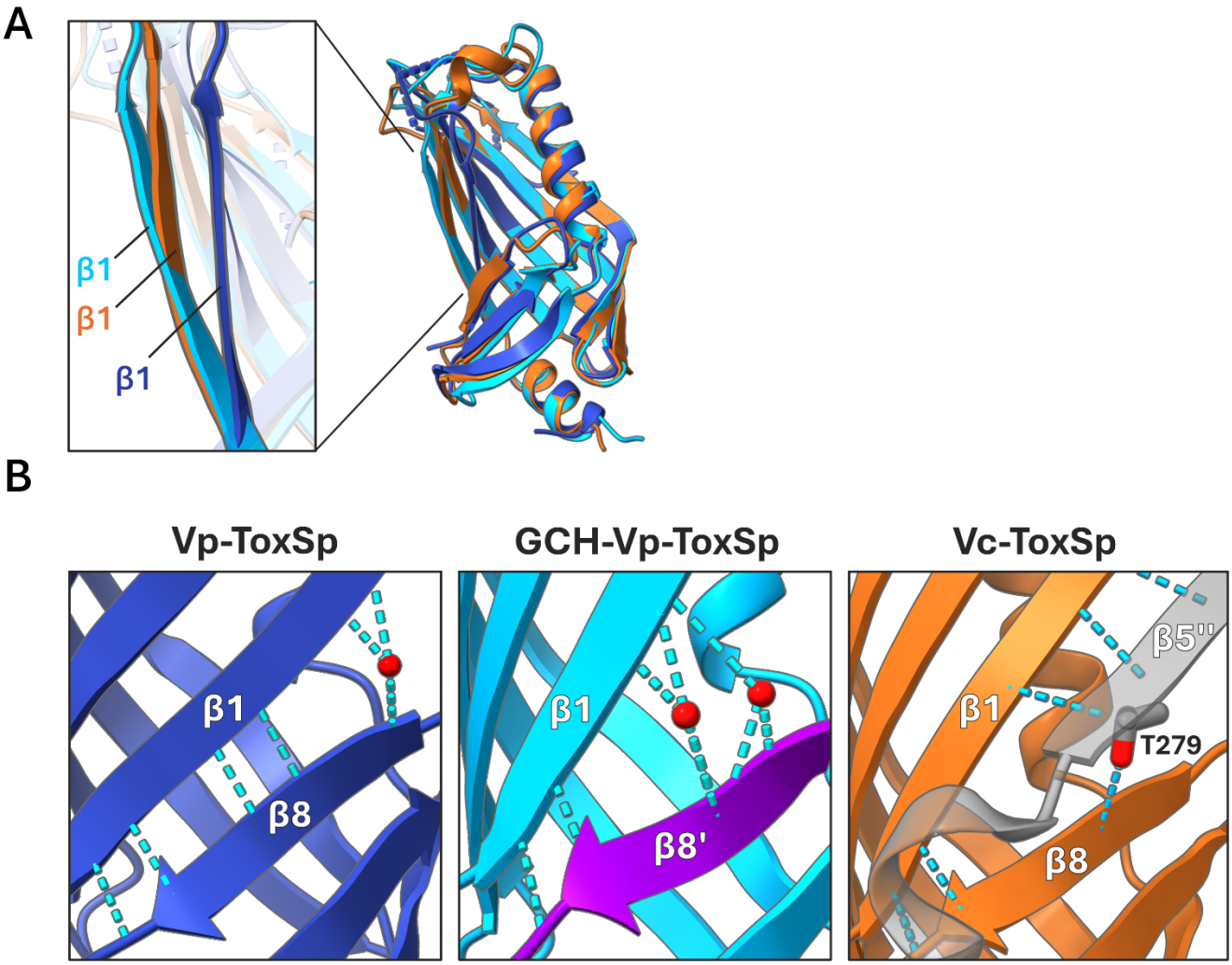

Figure 7. Structural comparison of apo Vp-ToxSp, glycocholate-bound Vp-ToxSp, and Vc-ToxSp reveals bile- and ToxR-induced opening of the β-barrel. (A) Overlay of apo Vp-ToxSp (blue; PDB ID: 8U2F), glycocholate-bound (GCH) Vp-ToxSp monomer (cyan; PDB: 9ZJO, ligand omitted for clarity), and Vc-ToxSp from the heterodimeric ToxR-ToxS complex (orange; PDB: 8ALO). The comparison shows that apo Vp-ToxSp adopts a more closed conformation, whereas both glycocholate-bound Vp-ToxSp and Vc-ToxSp display a more open conformation. (B) In apo Vp-ToxSp (left), a single water molecule bridges β1 and β8 strands to stabilize the closed conformation. In glycocholate-bound Vp-ToxSp (middle), two water molecules bind the more open interface, whereas in Vc-ToxSp (right), the corresponding position is occupied by the side chain of Thr279 from Vc-ToxRp.

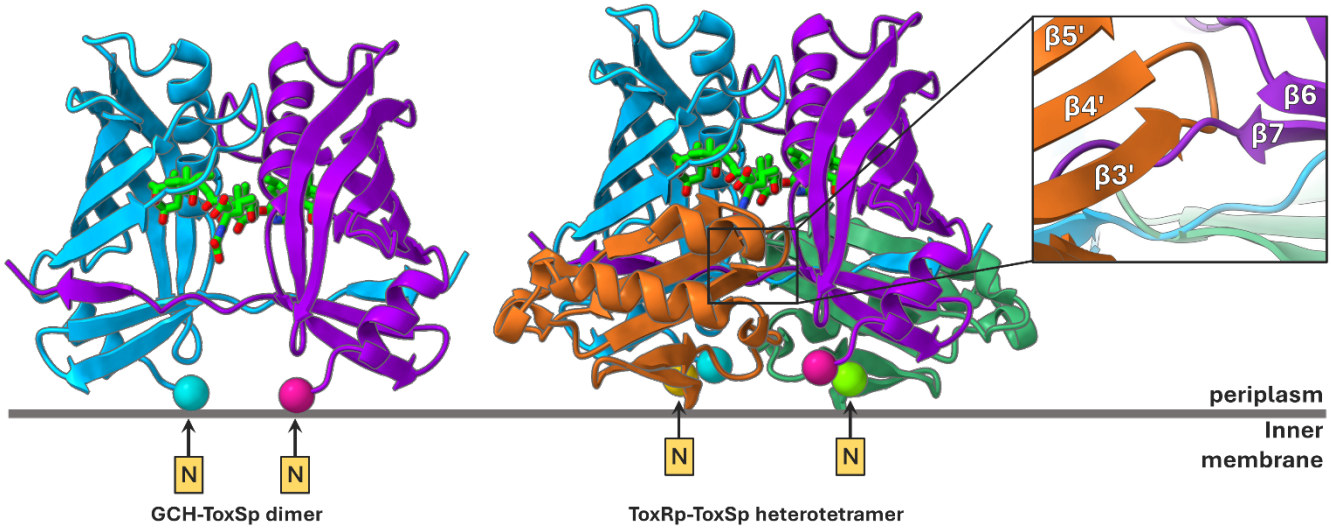

Figure 8. Model of the Vp-ToxSp-Vc-ToxRp heterotetramer. The model was generated using the Vp-ToxSp homodimer described in this study and then positioning the two Vc-ToxRp chains using the *V. cholerae* ToxRS heterodimer (PDB: 8ALO) to build the heterotetramer. This model positions the periplasmic domains of ToxS and ToxR in a physiologically plausible orientation with all four N-termini facing the membrane and minimal steric clashes between ToxR and ToxS.

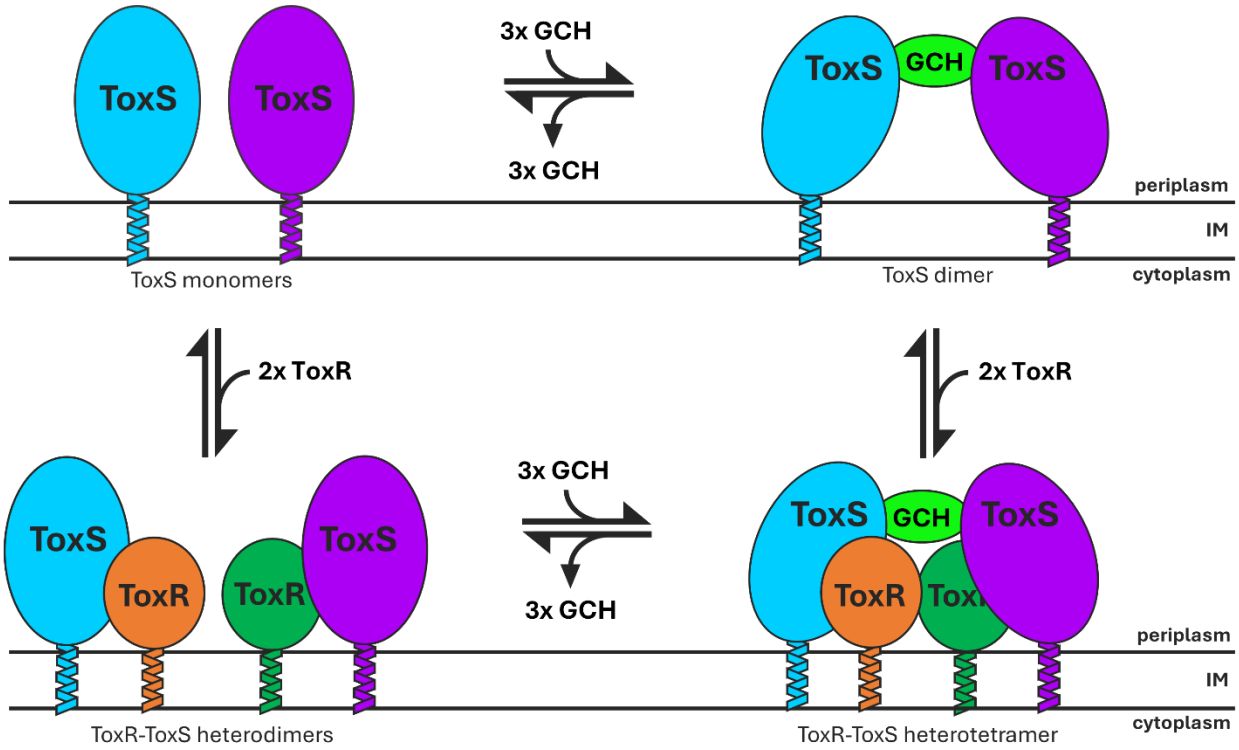

Figure 9. Model for the bile-induced activation of ToxRS. Monomeric, apo ToxS (upper left) forms a domain-swapped homodimer upon glycocholate binding (upper right). Conformational changes induced by ligand binding and dimerization favor ToxR binding, resulting in an active heterotetramer that can bind DNA (lower right). Alternatively, glycocholate binding to apo ToxRS dimers (lower left) induces heterotetramer formation.

Reference:

Adams, P. D., Afonine, P. V., Bunkóczi, G., Chen, V. B., Davis, I. W., Echols, N., Headd, J. J., Hung, L. W., Kapral, G. J., Grosse-Kunstleve, R. W., McCoy, A. J., Moriarty, N. W., Oeffner, R., Read, R. J., Richardson, D. C., Richardson, J. S., Terwilliger, T. C., & Zwart, P. H. (2010). PHENIX: a comprehensive Python-based system for macromolecular structure solution. *Acta Crystallographica. Section D, Biological Crystallography*, *66*(Pt 2), 213–221. https://doi.org/10.1107/S0907444909052925

Almagro-Moreno, S., Root, M. Z., & Taylor, R. K. (2015). Role of ToxS in the proteolytic cascade of virulence regulator ToxR in Vibrio cholerae. *Molecular Microbiology*, *98*(5), 963–976. https://doi.org/10.1111/mmi.13170

Altschul, S. F., Gish, W., Miller, W., Myers, E. W., & Lipman, D. J. (1990). Basic local alignment search tool. *Journal of Molecular Biology*, *215*(3), 403–410. https://doi.org/10.1016/S0022-2836(05)80360-2

Beck, N. A., Krukonis, E. S., & DiRita, V. J. (2004). TcpH influences virulence gene expression in Vibrio cholerae by inhibiting degradation of the transcription activator TcpP. *Journal of Bacteriology*, *186*(24), 8309–8316. https://doi.org/10.1128/JB.186.24.8309-8316.2004

Canals, A., Pieretti, S., Muriel-Masanes, M., El Yaman, N., Plecha, S. C., Thomson, J. J., Fàbrega-Ferrer, M., Pérez-Luque, R., Krukonis, E. S., & Coll, M. (2023). ToxR activates the Vibrio cholerae virulence genes by tethering DNA to the membrane through versatile binding to multiple sites. *Proceedings of the National Academy of Sciences of the United States of America*, *120*(29), e2304378120. https://doi.org/10.1073/PNAS.2304378120

Crawford, J. A., Kaper, J. B., & DiRita, V. J. (1998). Analysis of ToxR-dependent transcription activation of ompU, the gene encoding a major envelope protein in Vibrio cholerae. *Molecular Microbiology*, *29*(1), 235–246. https://doi.org/10.1046/J.1365-2958.1998.00925.X

Crawford, J. A., Krukonis, E. S., & DiRita, V. J. (2003). Membrane localization of the ToxR winged-helix domain is required for TcpP-mediated virulence gene activation in Vibrio cholerae. *Molecular Microbiology*, *47*(5), 1459–1473. https://doi.org/10.1046/J.1365-2958.2003.03398.X

Demey, L. M., Gumerov, V. M., Xing, J., Zhulin, I. B., & DiRita, V. J. (2023). Transmembrane Transcription Regulators Are Widespread in Bacteria and Archaea. *Microbiology Spectrum*, *11*(3), 1–13. https://doi.org/10.1128/spectrum.00266-23

DiRita, V. J., & Mekalanos, J. J. (1991). Periplasmic interaction between two membrane regulatory proteins, ToxR and ToxS, results in signal transduction and transcriptional activation. *Cell*, *64*(1), 29–37. https://doi.org/10.1016/0092-8674(91)90206-E

DiRita, V., Parsot, C., Jander, G., & Mekalanos, J. (1991). Regulatory cascade controls virulence in Vibrio cholerae. *Proceedings of the National Academy of Sciences of the United States of America*, *88*(12), 5403–5407. https://doi.org/10.1073/PNAS.88.12.5403

Emsley, P., & Cowtan, K. (2004). Coot: model-building tools for molecular graphics. *Acta Crystallographica. Section D, Biological Crystallography*, *60*(Pt 12 Pt 1), 2126–2132. https://doi.org/10.1107/S0907444904019158

Fengler, V. H. I., Boritsch, E. C., Tutz, S., Seper, A., Ebner, H., Roier, S., Schild, S., & Reidl, J. (2012). Disulfide Bond Formation and ToxR Activity in Vibrio cholerae. *PLoS ONE*, *7*(10), 47756. https://doi.org/10.1371/journal.pone.0047756

Fränzel, B., Penkova, M., Frese, C., Metzler-Nolte, N., & Andreas Wolters, D. (2012). Escherichia coli exhibits a membrane-related response to a small arginine- and tryptophan-rich antimicrobial peptide. *Proteomics*, *12*(14), 2319–2330. https://doi.org/10.1002/PMIC.201100636

Gao, X., Zhang, Z., Qian, Q., Chen, Q., Gu, S., Li, J., Zhang, Y., Wu, C., Jiang, Q., & Zhang, X. (2022). Survival Characteristics and Transcriptomic Analyses Reveal the Adaptive Response of the Aquatic Pathogen Non-O1/O139 Vibrio cholerae to Starvation Stress. *Microbiology Spectrum*, *10*(3). https://doi.org/10.1128/SPECTRUM.01939-21

Gotoh, K., Kodama, T., Hiyoshi, H., Izutsu, K., Park, K. S., Dryselius, R., Akeda, Y., Honda, T., & Iida, T. (2010). Bile acid-induced virulence gene expression of Vibrio parahaemolyticus reveals a novel therapeutic potential for bile acid sequestrants. *PloS One*, *5*(10). https://doi.org/10.1371/JOURNAL.PONE.0013365

Gubensäk, N., Sagmeister, T., Buhlheller, C., Geronimo, B. D., Wagner, G. E., Petrowitsch, L., Gräwert, M., Rotzinger, M., Berger, T. M. I., Schäfer, J., Usón, I., Reidl, J., Sánchez-Murcia, P. A., Zangger, K., & Pavkov-Keller, T. (2023). Vibrio cholerae's ToxRS Bile Sensing System. *ELife*, *12*. https://doi.org/10.7554/ELIFE.88721

Herrington, D. A., Hall, R. H., Losonsky, G., Mekalanos, J. J., Taylor, R. K., & Levine, M. M. (1988). Toxin, toxin-coregulated pili, and the toxR regulon are essential for Vibrio cholerae pathogenesis in humans. *The Journal of Experimental Medicine*, *168*(4), 1487–1492. https://doi.org/10.1084/JEM.168.4.1487

Higgins, D. E., & DiRita, V. J. (1994). Transcriptional control of toxT, a regulatory gene in the ToxR regulon of Vibrio cholerae. *Molecular Microbiology*, *14*(1), 17–29. https://doi.org/10.1111/J.1365-2958.1994.TB01263.X

Holm, L., & Laakso, L. M. (2016). Dali server update. *Nucleic Acids Research*, *44*(W1), W351–W355. https://doi.org/10.1093/NAR/GKW357

Hubbard, T. P., Chao, M. C., Abel, S., Blondel, C. J., Wiesch, P. A. Zur, Zhou, X., Davis, B. M., & Waldor, M. K. (2016). Genetic analysis of vibrio parahaemolyticus intestinal colonization. *Proceedings of the National Academy of Sciences of the United States of America*, *113*(22), 6283–6288. https://doi.org/10.1073/PNAS.1601718113

Jumper, J., Evans, R., Pritzel, A., Green, T., Figurnov, M., Ronneberger, O., Tunyasuvunakool, K., Bates, R., Žídek, A., Potapenko, A., Bridgland, A., Meyer, C., Kohl, S. A. A., Ballard, A. J., Cowie, A., Romera-Paredes, B., Nikolov, S., Jain, R., Adler, J., … Hassabis, D. (2021). Highly accurate protein structure prediction with AlphaFold. *Nature*, *596*(7873), 583–589. https://doi.org/10.1038/S41586-021-03819-2

Kabsch, W. (2010). XDS. *Acta Crystallographica Section D: Biological Crystallography*, *66*(Pt 2), 125. https://doi.org/10.1107/S0907444909047337

Kinch, L. N., Cong, Q., Jaishankar, J., & Orth, K. (2022). Co-component signal transduction systems: Fast-evolving virulence regulation cassettes discovered in enteric bacteria. *Proceedings of the National Academy of Sciences of the United States of America*, *119*(24). https://doi.org/10.1073/pnas.2203176119

Krishna, R., Wang, J., Ahern, W., Sturmfels, P., Venkatesh, P., Kalvet, I., Lee, G. R., Morey-Burrows, F. S., Anishchenko, I., Humphreys, I. R., McHugh, R., Vafeados, D., Li, X., Sutherland, G. A., Hitchcock, A., Neil Hunter, C., Kang, A., Brackenbrough, E., Bera, A. K., … Baker, D. (2024). Generalized biomolecular modeling and design with RoseTTAFold All-Atom. *Science*, *384*(6693). https://doi.org/10.1126/SCIENCE.ADL2528

Krukonis, E. S., Yu, R. R., & DiRita, V. J. (2000). The Vibrio cholerae ToxR/TcpP/ToxT virulence cascade: Distinct roles for two membrane-localized transcriptional activators on a single promoter. *Molecular Microbiology*, *38*(1), 67–84. https://doi.org/10.1046/j.1365-2958.2000.02111.x

Lario, P. I., Pfuetzner, R. A., Frey, E. A., Creagh, L., Haynes, C., Maurelli, A. T., & Strynadka, N. C. J. (2005). Structure and biochemical analysis of a secretin pilot protein. *The EMBO Journal*, *24*(6), 1111–1121. https://doi.org/10.1038/SJ.EMBOJ.7600610

Lee, S. E., Shin, S. H., Kim, S. Y., Kim, Y. R., Shin, D. H., Chung, S. S., Lee, Z. H., Lee, J. Y., Jeong, K. C., Choi, S. H., & Rhee, J. H. (2000). Vibrio vulnificus has the transmembrane transcription activator ToxRS stimulating the expression of the hemolysin gene vvhA. *Journal of Bacteriology*, *182*(12), 3405–3415. https://doi.org/10.1128/JB.182.12.3405-3415.2000

Lembke, M., Pennetzdorfer, N., Tutz, S., Koller, M., Vorkapic, D., Zhu, J., Schild, S., & Reidl, J. (2018). Proteolysis of ToxR is controlled by cysteine-thiol redox state and bile salts in Vibrio cholerae. *Molecular Microbiology*, *110*(5), 796–810. https://doi.org/10.1111/MMI.14125

Li, C. C., Crawford, J. A., DiRita, V. J., & Kaper, J. B. (2000). Molecular cloning and transcriptional regulation of ompT, a ToxR-repressed gene in Vibrio cholerae. *Molecular Microbiology*, *35*(1), 189–203. https://doi.org/10.1046/J.1365-2958.2000.01699.X

Li, P., Rivera-Cancel, G., Kinch, L. N., Salomon, D., Tomchick, D. R., Grishin, N. V., & Orth, K. (2016). Bile salt receptor complex activates a pathogenic type III secretion system. *ELife*, *5*(2016JULY). https://doi.org/10.7554/eLife.15718

Lilic, M., Jovanovic, M., Jovanovic, G., & Savic, D. J. (2003). Identification of the CysB-regulated gene, hslJ, related to the Escherichia coli novobiocin resistance phenotype. *FEMS Microbiology Letters*, *224*(2), 239–246. https://doi.org/10.1016/S0378-1097(03)00441-5,

Madeira, F., Madhusoodanan, N., Lee, J., Eusebi, A., Niewielska, A., Tivey, A. R. N., Lopez, R., & Butcher, S. (2024). The EMBL-EBI Job Dispatcher sequence analysis tools framework in 2024. *Nucleic Acids Research*, *52*(W1), W521–W525. https://doi.org/10.1093/NAR/GKAE241

Mey, A. R., Craig, S. A., & Payne, S. M. (2012). Effects of amino acid supplementation on porin expression and ToxR levels in Vibrio cholerae. *Infection and Immunity*, *80*(2), 518–528. https://doi.org/10.1128/IAI.05851-11

Midgett, C. R., Almagro-Moreno, S., Pellegrini, M., Taylor, R. K., Skorupski, K., & Kull, F. J. (2017). Bile salts and alkaline pH reciprocally modulate the interaction between the periplasmic domains of Vibrio cholerae ToxR and ToxS. *Molecular Microbiology*, *105*(2), 258–272. https://doi.org/10.1111/mmi.13699

Midgett, C. R., Swindell, R. A., Pellegrini, M., & Kull, F. J. (2020). A disulfide constrains the ToxR periplasmic domain structure, altering its interactions with ToxS and bile-salts. *Scientific Reports, 10*(1), 1–11. https://doi.org/10.1038/s41598-020-66050-5

Miller, K. A., Sofia, M. K., Weaver, J. W. A., Seward, C. H., & Dziejman, M. (2016). Regulation by ToxR-Like Proteins Converges on vttRB Expression To Control Type 3 Secretion System-Dependent Caco2-BBE Cytotoxicity in Vibrio cholerae. *Journal of Bacteriology*, *198*(11), 1675. https://doi.org/10.1128/JB.00130-16

Miller, V. L., DiRita, V. J., & Mekalanos, J. J. (1989). Identification of toxS, a regulatory gene whose product enhances ToxR-mediated activation of the cholera toxin promoter. *Journal of Bacteriology*, *171*(3), 1288–1293. https://doi.org/10.1128/jb.171.3.1288-1293.1989

Miller, V. L., & Mekalanos, J. J. (1984). Synthesis of cholera toxin is positively regulated at the transcriptional level by toxR. *Proceedings of the National Academy of Sciences of the United States of America*, *81*(11), 3471–3475. https://doi.org/10.1073/PNAS.81.11.3471

Morgan, J. K., Carroll, R. K., Harro, C. M., Vendura, K. W., Shaw, L. N., & Riordan, J. T. (2015). Global Regulator of Virulence A (GrvA) Coordinates Expression of Discrete Pathogenic Mechanisms in Enterohemorrhagic Escherichia coli through Interactions with GadW-GadE. *Journal of Bacteriology*, *198*(3), 394–409. https://doi.org/10.1128/JB.00556-15

Morgan, S. J., Felek, S., Gadwal, S., Koropatkin, N. M., Perry, J. W., Bryson, A. B., & Krukonis, E. S. (2011). The two faces of ToxR: activator of ompU, co-regulator of toxT in Vibrio cholerae. *Molecular Microbiology*, *81*(1), 113–128. https://doi.org/10.1111/J.1365-2958.2011.07681.X

Okon, M., Moraes, T. F., Lario, P. I., Creagh, A. L., Haynes, C. A., Strynadka, N. C. J., & McIntosh, L. P. (2008). Structural Characterization of the Type-III Pilot-Secretin Complex from Shigella flexneri. *Structure*, *16*(10), 1544–1554. https://doi.org/10.1016/j.str.2008.08.006

Okonechnikov, K., Golosova, O., Fursov, M., Varlamov, A., Vaskin, Y., Efremov, I., German Grehov, O. G., Kandrov, D., Rasputin, K., Syabro, M., & Tleukenov, T. (2012). Unipro UGENE: a unified bioinformatics toolkit. *Bioinformatics (Oxford, England)*, *28*(8), 1166–1167. https://doi.org/10.1093/BIOINFORMATICS/BTS091

Ottemann, K. M., & Mekalanos, J. J. (1996). The ToxR protein of Vibrio cholerae forms homodimers and heterodimers. *Journal of Bacteriology*, *178*(1), 156–162. https://doi.org/10.1128/JB.178.1.156-162.1996

Pearson, G. D. N., DiRita, V. J., Goldberg, M. B., Boyko, S. A., Calderwood, S. B., & Mekalanos, J. J. (1990). New attenuated derivatives of Vibrio cholerae. *Research in Microbiology*, *141*(7–8), 893–899. https://doi.org/10.1016/0923-2508(90)90127-C

Pei, J., & Grishin, N. V. (2001). AL2CO: calculation of positional conservation in a protein sequence alignment. *Bioinformatics (Oxford, England)*, *17*(8), 700–712. https://doi.org/10.1093/BIOINFORMATICS/17.8.700

Pettersen, E. F., Goddard, T. D., Huang, C. C., Couch, G. S., Greenblatt, D. M., Meng, E. C., & Ferrin, T. E. (2004). UCSF Chimera--a visualization system for exploratory research and analysis. *Journal of Computational Chemistry*, *25*(13), 1605–1612. https://doi.org/10.1002/JCC.20084

Pfau, J. D., & Taylor, R. K. (1998). Mutations in toxR and toxS that separate transcriptional activation from DNA binding at the cholera toxin gene promoter. *Journal of Bacteriology*, *180*(17), 4724–4733. https://doi.org/10.1128/JB.180.17.4724-4733.1998

Provenzano, D., Schuhmacher, D. A., Barker, J. L., & Klose, K. E. (2000). The virulence regulatory protein ToxR mediates enhanced bile resistance in Vibrio cholerae and other pathogenic Vibrio species. *Infection and Immunity*, *68*(3), 1491–1497. https://doi.org/10.1128/IAI.68.3.1491-1497.2000

Puri, V., Goyal, A., Sankaranarayanan, R., Enright, A. J., & Vaidya, T. (2011). Evolutionary and functional insights into Leishmania META1: Evidence for lateral gene transfer and a role for META1 in secretion. *BMC Evolutionary Biology*, *11*(1), 1–17. https://doi.org/10.1186/1471-2148-11-334

Quinn, J. D., Weening, E. H., Miner, T. A., & Miller, V. L. (2019). Temperature Control of psaA Expression by PsaE and PsaF in Yersinia pestis. *Journal of Bacteriology*, *201*(16). https://doi.org/10.1128/JB.00217-19

Ramos, C. S., Yokoyama-Yasunaka, J. K. U., Guerra-Giraldez, C., Price, H. P., Mortara, R. A., Smith, D. F., & Uliana, S. R. B. (2011). Leishmania amazonensis META2 protein confers protection against heat shock and oxidative stress. *Experimental Parasitology*, *127*(1), 228–237. https://doi.org/10.1016/j.exppara.2010.08.004

Reich, K. A., & Schoolnik, G. K. (1994). The light organ symbiont Vibrio fischeri possesses a homolog of the Vibrio cholerae transmembrane transcriptional activator ToxR. *Journal of Bacteriology*, *176*(10), 3085–3088. https://doi.org/10.1128/JB.176.10.3085-3088.1994

Sayers, E. W., Beck, J., Bolton, E. E., Brister, J. R., Chan, J., Comeau, D. C., Connor, R., DiCuccio, M., Farrell, C. M., Feldgarden, M., Fine, A. M., Funk, K., Hatcher, E., Hoeppner, M., Kane, M., Kannan, S., Katz, K. S., Kelly, C., Klimke, W., … Sherry, S. T. (2024). Database resources of the National Center for Biotechnology Information. *Nucleic Acids Research*, *52*(D1), D33–D43. https://doi.org/10.1093/NAR/GKAD1044

Schaeffer, R. D., Medvedev, K. E., Andreeva, A., Chuguransky, S. R., Pinto, B. L., Zhang, J., Cong, Q., Bateman, A., & Grishin, N. V. (2025). ECOD: integrating classifications of protein domains from experimental and predicted structures. *Nucleic Acids Research*, *53*(D1), D411–D418. https://doi.org/10.1093/NAR/GKAE1029

Schuch, R., & Maurelli, A. T. (1999). The Mxi-Spa Type III Secretory Pathway of Shigella flexneri Requires an Outer Membrane Lipoprotein, MxiM, for Invasin Translocation. *Infection and Immunity*, *67*(4), 1982. https://doi.org/10.1128/IAI.67.4.1982-1991.1999

Schuch, R., & Maurelli, A. T. (2001). MxiM and MxiJ, Base Elements of the Mxi-Spa Type III Secretion System of Shigella, Interact with and Stabilize the MxiD Secretin in the Cell Envelope. *Journal of Bacteriology*, *183*(24), 6991. https://doi.org/10.1128/JB.183.24.6991-6998.2001

Scribano, D., Marzano, V., Mortera, S. L., Sarshar, M., Vernocchi, P., Zagaglia, C., Putignani, L., Palamara, A. T., & Ambrosi, C. (2019). Insights into the Periplasmic Proteins of Acinetobacter baumannii AB5075 and the Impact of Imipenem Exposure: A Proteomic Approach. *International Journal of Molecular Sciences*, *20*(14). https://doi.org/10.3390/IJMS20143451

Scribano, D., Pasqua, M., Limongi, D., Nencioni, L., Palamara, A. T., & Ambrosi, C. (2025). The periplasmic protein HslJ is the first-line of defense against oxidative stress in Acinetobacter baumannii. *Biological Research*, *58*(1), 2. https://doi.org/10.1186/S40659-025-00584-8

Sievers, F., Wilm, A., Dineen, D., Gibson, T. J., Karplus, K., Li, W., Lopez, R., McWilliam, H., Remmert, M., Söding, J., Thompson, J. D., & Higgins, D. G. (2011). Fast, scalable generation of high-quality protein multiple sequence alignments using Clustal Omega. *Molecular Systems Biology*, *7*, 539. https://doi.org/10.1038/MSB.2011.75

Studier, F. W. (2005). Protein production by auto-induction in high density shaking cultures. *Protein Expression and Purification*, *41*(1), 207–234. https://doi.org/10.1016/j.pep.2005.01.016

Vagin, A. A., Steiner, R. A., Lebedev, A. A., Potterton, L., McNicholas, S., Long, F., & Murshudov, G. N. (2004). REFMAC5 dictionary: Organization of prior chemical knowledge and guidelines for its use. *Acta Crystallographica Section D: Biological Crystallography*, *60*(12 I), 2184–2195. https://doi.org/10.1107/S0907444904023510

Vonrhein, C., Flensburg, C., Keller, P., Sharff, A., Smart, O., Paciorek, W., Womack, T., & Bricogne, G. (2011). Data processing and analysis with the autoPROC toolbox. *Urn:Issn:0907-4449*, *67*(4), 293–302. https://doi.org/10.1107/S0907444911007773

Welch, T. J., & Bartlett, D. H. (1998). Identification of a regulatory protein required for pressure-responsive gene expression in the deep-sea bacterium Photobacterium species strain SS9. *Molecular Microbiology*, *27*(5), 977–985. https://doi.org/10.1046/J.1365-2958.1998.00742.X,

Withey, J. H., & DiRita, V. J. (2006). The toxbox: specific DNA sequence requirements for activation of Vibrio cholerae virulence genes by ToxT. *Molecular Microbiology*, *59*(6), 1779–1789. https://doi.org/10.1111/J.1365-2958.2006.05053.X

Xue, M., Xiao, Y., Fu, D., Raheem, M. A., Shao, Y., Song, X., Tu, J., Xue, T., & Qi, K. (2020). Transcriptional Regulator YqeI, Locating at ETT2 Locus, Affects the Pathogenicity of Avian Pathogenic Escherichia coli. *Animals : An Open Access Journal from MDPI*, *10*(9), 1658. https://doi.org/10.3390/ANI10091658

Zou, A. J., Kinch, L., Chimalapati, S., Garcia, N., Tomchick, D. R., & Orth, K. (2023). Molecular determinants for differential activation of the bile acid receptor from the pathogen Vibrio parahaemolyticus. *The Journal of Biological Chemistry*, *299*(4), 104591. https://doi.org/10.1016/J.JBC.2023.104591